A&A 376, 460–475 (2001)
DOI: 10.1051/0004-6361:20010879

Astronomy & Astrophysics

Multi-frequency variations of the Wolf-Rayet system HD 193793 (WC7pd+O4-5)

III. IUE observations

D. Y. A. Setia Gunawan[1,2,3], K. A. van der Hucht[2], P. M. Williams[4], H. F. Henrichs[5], L. Kaper[5], D. J. Stickland[6], and W. Wamsteker[7]

[1] Kapteyn Astronomical Institute, PO Box 800, 9700 AV Groningen, The Netherlands
e-mail: diah@astro.rug.nl
[2] Space Research Organization Netherlands, Sorbonnelaan 2, 3584 CA Utrecht, The Netherlands
[3] present address: Australia Telescope National Facility, PO Box 76, Epping, NSW 1710, Australia
[4] Institute for Astronomy, University of Edinburgh, Royal Observatory, Blackford Hill, Edinburgh EH9 3HJ, UK
e-mail: p.m.williams@roe.ac.uk
[5] Astronomical Institute *Anton Pannekoek*, University of Amsterdam, Kruislaan 403, 1098 SJ Amsterdam, The Netherlands
e-mail: huib;lexk@astro.uva.nl
[6] Space Science Department, Rutherford Appleton Observatory, Chilton, Didcot, Oxon OX11 OQX, UK
e-mail: ds@astro1.bnsc.rl.ac.uk
[7] ESA-IUE Observatory, VILSPA, PO Box 50727, 28080 Madrid, Spain
e-mail: wwamstek@notes.vilspa.esa.es

Received 20 February 2001 / Accepted 15 June 2001

Abstract. The colliding-wind binary system WR 140 (HD 193793, WC7pd+O4-5, $P = 7.94$ yr) was monitored in the ultraviolet by *IUE* from 1979 to 1994 in 35 short-wavelength high-resolution spectra. An absorption-line radial-velocity solution is obtained from the photospheric lines of the O component, by comparison with a single O star. The resulting orbital parameters, $e = 0.87 \pm 0.05$, $\omega = 31° \pm 9°$ and $K_{\rm O\,star} = 25 \pm 15$ km s^{-1}, confirm the large eccentricity of the orbit, within the uncertainties of previous optical studies. This brings the weighted mean UV-optical eccentricity to $e = 0.85 \pm 0.04$. Occultation of the O-star light by the WC wind and the WC+O colliding-wind region results into orbital modulation of the P-Cygni profiles of the C II, C IV and Si IV resonance lines. Near periastron passage, the absorption troughs of those resonance-line profiles increase abruptly in strength and width, followed by a gradual decrease. In particular, near periastron the *blue* black-edges of the P-Cygni absorption troughs shift to larger outflow velocities. We discuss that the apparently larger wind velocity and velocity dispersion observed at periastron could be explained by four phenomena: (*i*) geometrical resonance-line eclipse effects being the main cause of the observed UV spectral variability, enhanced by sightline crossing of the turbulent wind-wind collision zone; (*ii*) the possibility of an orbital-plane enhanced WC7 stellar wind; (*iii*) possible common-envelope acceleration by the combined WC and O stellar radiation fields; and (*iv*) possible enhanced radiatively driven mass loss due to tidal stresses, focused along the orbiting line of centers.

Key words. stars: binaries: spectroscopic – stars: early-type – stars: Wolf-Rayet – stars: individual: WR 140 – stars: winds, outflows – ultraviolet: stars

1. Introduction

Wolf-Rayet (WR) stars are massive stars characterized by strong stellar winds, driving mass-loss rates of the order of $10^{-5}\,M_\odot$ yr^{-1} (viz., van der Hucht 1992). In the case of WR+OB binary systems, wind-wind collision causes heating and compression where the WR and OB wind momenta match. In case of eccentric binary orbits, the change in binary separation of, and in lines-of-sight to, the two binary components cause variability in several wavelength domains: X-ray flux variability, ultraviolet line-profile variability, infrared flux variability in case of episodic dust formation, and non-thermal radio flux variability.

WR 140 (HD 193793, V1687 Cyg, van der Hucht et al. 1981; van der Hucht 2001) is a spectroscopic WC7 binary system with a O4-5 companion (according to Arnal (2001) possibly escaped from a triple system some

Send offprint requests to: K. A. van der Hucht,
e-mail: k.a.van.der.hucht@sron.nl

1.3×10^5 yr ago), for which the difficulties in finding a reliable radial-velocity solution have puzzled many observers (e.g., McDonald 1947; Conti 1971; Cherepashchuk 1976; Lamontagne et al. 1984; Conti et al. 1984). First classified as a WR star by Fleming (1889), its variability has drawn attention only since the 1970s. Discovery papers are: Schumann & Seggewiss (1975) on optical spectral variability; Hackwell et al. (1976) on infrared photometric variability; Florkowski & Gottesman (1977) on radio variability; Moffat & Shara (1986) on optical photometric variability; and Williams et al. (1987) on its combined IR, UV and X-ray variability linked to its spectroscopic orbit.

As to continuum variations, Williams et al. (1990, hereafter Paper I) searched for UV continuum variations in the then available *IUE* spectra of WR 140, but found none. At optical wavelengths, Moffat & Shara (1986) found micro-variability in broadband B observations of WR 140 obtained in a time span of 14 days, with an amplitude of 0.02 mag and a tentative period of $P = 6.25$ d. More recently, Panov et al. (2000) monitored WR 140 from 1991 to 1998 in *UBV* photometry. In 1993, a dip in the light curve in all passbands has been observed around periastron passage (see below), with a V-amplitude of 0.03 mag. They interpreted this dip in terms of an "eclipse" by dust condensation in the WC wind, of the type reported by Veen et al. (1998) for a number of late WC stars.

Thanks to the development of IR photometry in the early 1970s, unexpected IR variability of WR 140 was discovered. The 7.9 yr interval between two IR excesses was proven in a radial-velocity solution by Williams et al. (1987) to be the orbital period of an eccentric ($e = 0.84$) binary, with the IR excesses due to periodic dust formation around periastron passage. This motivated the classification WC7pd (van der Hucht 2001). The infrared, radio and X-ray observations were linked to a refined orbit by Williams et al. (1990: Paper I). Another IR excess of WR 140 occurred at the predicted time in March 1993 (Williams 1995; 2001).

Annuk (1995) measured the radial velocities of absorption lines and the C IV λ 4650 Å emission line. Combining his observational result and those of others, he derived a period of 2893 d. Annuk's absorption-line solution confirmed the orbital elements derived in Paper I with a slightly larger eccentricity, $e = 0.85 \pm 0.01$.

Radio studies of WR 140, also showing the 7.94 yr period, were published by Williams et al. (1994, hereafter Paper II) and by White & Becker (1995).

The observations mentioned above lead to a model for WR 140 of a WC7pd+O4-5 binary with interacting stellar winds forming two shock fronts with a contact discontinuity in between (see Papers I and II). Since the ratio of the wind momenta $\eta = \dot{M} v_\infty(\mathrm{WC7}) \,/\, \dot{M} v_\infty(\mathrm{O4\text{-}5}) \simeq 33$, the cone-shaped contact discontinuity is formed relatively close to the O component, with an opening angle depending on the value of η. Applying the orbital elements derived in Paper I, the O component is, in the line-of-sight, "behind" the WC star roughly at phases $0 < \phi < 0.1$ (see Fig. 2; periastron defines $\phi = 0$). In this phase range, the sightline (assuming an inclination $i \gtrsim 60°$) to the O component passes through the densest part of the WC and O stellar winds and their interaction region. Because in the UV the O component is ∼0.7 mag brighter than the WC component (Paper I), absorption in the sightline to the O component will dominate the P-Cygni absorption troughs in the spectrum of the WR 140 system in this phase range. The sightline to the O component is for about half of the orbit dominated by the WC7 wind.

Both the WC7 and O4-5 binary components of WR 140 have terminal wind velocities of the order of $v_\infty \simeq 3000$ km s^{-1}. Fitzpatrick et al. (1982) derived from the composite (WC7+O4-5) *IUE*-SWP 8004 spectrum of WR 140, that the C IV $\lambda\lambda$ 1548,1551 Å, Si IV $\lambda\lambda$ 1394,1403 Å and C III λ 1909 Å P-Cygni line profiles yield $v_\infty = 3000 \pm 100$ km s^{-1}. They also observed two narrow absorption features in the broad P-Cygni Si IV line. Since the spacing of these narrow absorption features is identical to the doublet spacing, they interpreted the narrow features as Si IV lines with a velocity of $v \simeq -2700$ km s^{-1}. Prinja et al. (1990) argued that the edge velocity ($v_{\rm black}$) of the saturated absorption part of P-Cygni profiles in high-resolution *IUE* spectra of OB and WR stars represented the terminal wind velocity, with on average $v_{\rm black} \simeq 0.76\, v_{\rm edge}$. From the composite (WC7+O4-5) *IUE*-SWP 31504 spectrum of WR 140, they measured for the resonance lines the wind velocities $v_{\rm CII} = 1510$ km s^{-1}, $v_{\rm SiIV} = 2640$ km s^{-1}, and $v_{\rm CIV} = 2900$ km s^{-1}. Eenens & Williams (1994) measured the terminal velocities of WR stars from the P-Cygni absorption components of the near-IR He I lines at $\lambda\, 1.083\, \mu$m and $\lambda\, 2.058\, \mu$m. They found that the observed He I terminal wind velocities correspond to about 70% of the violet-edge velocities of the UV resonance P-Cygni profiles of C IV and Si IV, agreeing well with $v_{\rm black}$ of the saturated absorption troughs. The terminal wind velocities that they derived for WR 140 were $v_{\rm HeI\,1.083\mu m} = 2900$ km s^{-1} and $v_{\rm HeI\,2.058\mu m} = 2845$ km s^{-1}, and were ascribed to the WC7 component.

The motivation for the present study was to monitor WR 140 for variations in the UV P-Cygni profiles of resonance lines of abundant ions as a function of orbital phase, and to obtain a UV radial velocity solution, the combination of both allowing us to interpret any observed variations as a function of orbital geometry, aspect angle, and varying lines-of-sight towards the binary components, and improving our understanding of the physical nature of the wind-wind interaction.

We present results of monitoring of WR 140 in the period 1978 to 1994 with the *International Ultraviolet Explorer* (*IUE*) short wavelength spectrograph. Observations and data reduction are described in Sect. 2. The analysis, in Sect. 3, includes (*i*) a radial-velocity study based on the O component absorption lines; (*ii*) a study of the continuum flux variations as a function of orbital phase; (*iii*) a study of the statistical significance of the observed line profile variability; and (*iv*) a study of the variability of the observed P-Cygni

profiles. In Sect. 4 the results are discussed, and Sect. 5 summarizes the conclusions.

Preliminary studies of these data were published by Setia Gunawan et al. (1995a; 1995b).

2. Observations and data reduction

WR 140 was observed with *IUE* from 1979 to 1994 in 35 SWP (short Wavelength Prime camera, $\lambda\lambda$ 1165–2126 Å, $\Delta\lambda \simeq 0.1$ Å) images, through the large aperture ($10'' \times 20''$), mostly in our own programs at the ESA-*IUE* Observatory in Villafranca, Spain, many of them as service observations.

Most *IUE*-SWP spectra were taken with an exposure time of 120 min; SWP data taken with an exposure time of 195 min show saturation and could not be used for the emission-line variability study, but were still useful to study the O-star absorption lines. Some spectra were recorded in shorter exposure times caused by time-loss during hand-over between the NASA and ESA ground-stations. The log of observations is presented in Table 1. The orbital phases were calculated from the weighted means of the orbital parameters resulting from this study and those of Paper I.

Table 1. Log of observations of WR 140 (WC7pd+O4-5) using the *IUE*-SWP camera. Phases ϕ have been calculated adopting $P = 2900$ d and the weighted mean of $T_{\rm periastron}$ from Paper I and this study. Julian dates represent mid-exposure times. The velocities refer to the O4-5 companion. *RV*: radial velocity. O–C: observed minus computed.

IUE-SWP number	JD 2 440 000+	$t_{\rm exp}$ (min)	ϕ	*RV* (km s^{-1})	O–C (km s^{-1})
6945	4168.659	70	0.315	17.8	–1.1
8004	4291.392	70	0.358	18.1	–1.2
9492	4431.433	195	0.406	23.3	3.5
25788	6182.845	60	0.010	19.1	1.0
27064	6379.234	70	0.078	13.6	–3.3
28111	6526.655	70	0.129	16.5	–0.7
29954	6788.988	85	0.219	17.6	–0.4
31504	7015.321	75	0.297	17.9	–0.8
33425	7283.600	120	0.390	19.2	–0.4
34064	7383.367	195	0.424	20.8	0.8
35886	7614.743	120	0.504	21.6	0.7
36834	7752.213	80	0.551	16.5	–4.9
37675	7855.045	120	0.587	21.7	–0.2
38581	7993.774	90	0.634	20.4	–2.3
38798	8027.741	120	0.646	23.8	0.9
39061	8053.660	117	0.655	24.0	1.0
39311	8100.363	120	0.671	21.0	–2.3
40201	8222.090	120	0.713	25.8	1.6
41451	8368.655	120	0.764	25.6	0.1
41977	8440.377	120	0.788	26.6	0.3
42319	8494.281	120	0.807	22.3	–4.6
42582	8529.256	110	0.819	31.0	3.5
43277	8591.218	107	0.840	37.7	9.1
43426	8610.147	120	0.847	32.9	4.0
44828	8775.473	120	0.904	34.3	–0.1
44965	8794.447	120	0.911	26.5	–9.1
45231	8830.465	120	0.923	42.5	4.0
45530	8871.210	120	0.937	50.1	6.3
46119	8929.235	120	0.957	59.3	–3.9
47470	9089.794	110	0.012	19.3	1.5
47727	9132.558	120	0.027	13.6	–3.7
48783	9259.224	120	0.071	16.9	0.0
49004	9285.142	120	0.080	21.3	4.4
49287	9313.078	120	0.089	20.8	3.8
50708	9479.635	120	0.147	20.4	3.0

The spectra were extracted from photometrically corrected PHOT-images, except the first two *IUE*-SWP spectra (SWP6945 and SWP8004) which were extracted from GPHOT-images, using the STARLINK IUEDR software package (Rees et al. 1996a, 1996b). After correction for order-overlap using the algorithm of Bianchi & Bohlin (1984), the wavelength shift was removed by aligning on several narrow interstellar lines. Subsequently, ripple-correction was applied to the *IUE*-SWP images following Barker (1984). The spectra were then mapped onto an equidistant wavelength grid with intervals of 0.1 Å. The flux in the resulting spectra is given in units of *IUE* Flux Number per second (FN/S). Absolute calibrated spectra can be retrieved from the INES system (Cassatella 2000).

Analysis of the data was performed by using the STARLINK DIPSO software package (Howarth et al. 1998). The gaps in the spectra caused by reseau marks were removed by three-point interpolation at either side of the gaps. This caused discontinuities in some spectra where the gaps are too wide. In those cases no interpolation was performed.

3. Analysis

3.1. Radial velocity study

For the purpose of measuring radial velocities of the absorption lines of the O component of the WR 140 system, we used a Cross-Correlation Function method (CCF, Stickland & Lloyd 1990). The *IUE*-SWP spectra of WR 140, aligned on interstellar lines, were compared with the archive *IUE* spectrum of the single O4V star HD 96715. The orbital parameters were derived by means of the program RVORBIT by Hill (DAO, private communication). The single-lined radial-velocity curve is shown in Fig. 1 and the resulting orbital parameters are listed in Table 2, Col. (3). We emphasize that this UV radial-velocity solution is independent from measurements and solutions at other wavelengths, apart from the adoption of the IR photometric period of $P = 2900$ d. In particular, the high velocities immediately preceding the 1993 periastron passage, which greatly influence the elements determined, were observed three cycles later than the corresponding (1969) optical data used for the solution in Paper I. Column (2) of Table 2 lists the orbital parameters of Paper I; we note the good correspondence. Column (4) lists the combined orbital parameters, weighted by $\sigma^{-0.5}$. The corresponding orbital phases per *IUE* observation are given in Table 1.

The position of the O star with respect to the WC star at the times of the *IUE* observations, on the basis of the averaged orbital parameters, is shown in Fig. 2. The figure demonstrates that owing to the large eccentricity, both

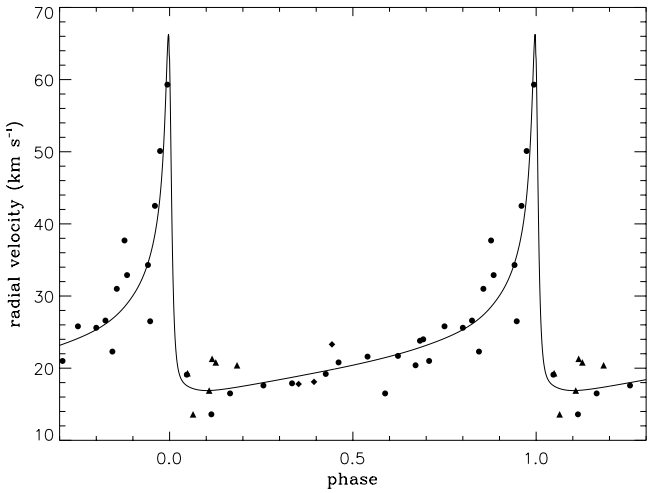

Fig. 1. The *IUE* UV single-lined (absorption-line) radial-velocity curve of the O4-5 companion of WR 140, applying as fixed period $P = 2900$ d, following Paper I. The data taken before the 1985.26 periastron passage are marked with ♦ symbols; those between the 1985.26 and 1993.2 periastron passages are marked with • symbols; and those after the 1993.2 periastron passage are marked with ▲ symbols. The ensuing orbital parameters are given in Table 2.

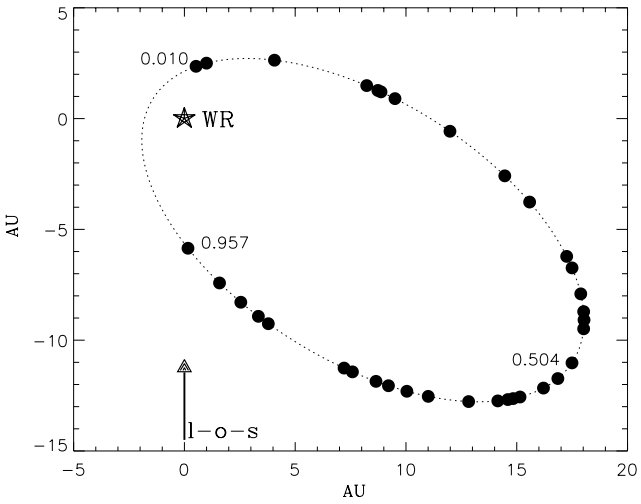

Fig. 2. The WR 140 binary orbit, showing the positions of the O-type component in the rest-frame of the WR component at the epochs of the *IUE* observations listed in Table 1. Orbital parameters e and ω are weighted means of this study and Paper I. The numbers next to the O star positions give the orbital phases.

conjunctions are very close to periastron passage, occurring at $\phi = 0.957$ (O star in front) and $\phi = 0.010$ (O star behind).

An attempt to measure the radial velocities of *emission* lines of the WC component of WR 140 by comparison with those of a single WC7 star, to obtain a double-lined radial-velocity solution, did not lead to significant results. This is due to line-width differences between individual WC7 stars and severe blending of WC7 emission lines.

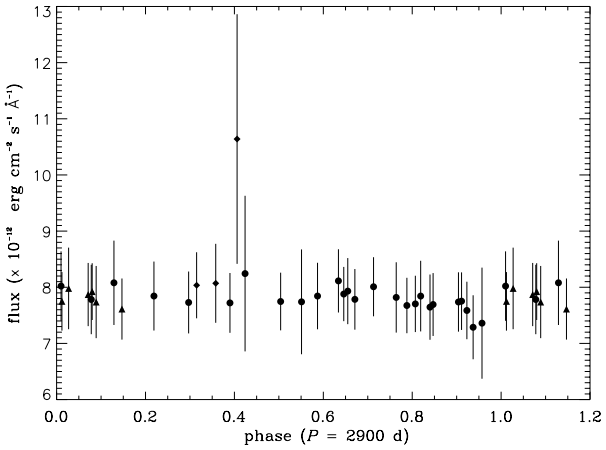

Fig. 3. Ultraviolet continuum fluxes from the absolute calibrated *IUE*-SWS high-resolution spectra of WR 140 in the wavelength region 1790–1800 Å. The excess point at $\phi = 0.406$ is due to overexposure. Symbols as in Fig. 1.

The eccentricity $e = 0.87 \pm 0.05$ derived in this study agrees well with the value 0.84 ± 0.04 calculated in Paper I from optical spectra. The UV data suggest that periastron passage occurs 104 ± 117 days earlier than derived in Paper I. The large error bar is caused by the limited amount of data obtained during periastron: we do not have sufficient coverage before the 1985 periastron (at phases $0.4 < \phi < 1.0$) and at the time of the 1993 periastron the position of WR 140 was violating the *IUE* Sun-constraint. Another indication that periastron occurs earlier, stems from the *ASCA* X-ray study of WR 140 by Zhekov & Skinner (2000), who argued that periastron occurs 72 days earlier than derived in Paper I.

Our least-squares fit of the radial-velocity curve has a relatively small rms-error of 3.5 km s^{-1}. From the orbital elements resulting from this UV radial-velocity study, we derive for the O-star orbit a semi-major axis $a_{\rm O} \sin i = 3.29$ AU and a mass function $f(M) = M_{\rm WR}^3 \sin^3 i \,/\, (M_{\rm WR} + M_{\rm O})^2 = 0.56\, M_\odot$. Assuming for the mass of the O4-5 component $M_{\rm O} = 38\, M_\odot$ (Paper I) and $i = 60°$ would imply that $M_{\rm WR} = 13\, M_\odot$.

3.2. The ultraviolet continuum flux

As discussed earlier in Paper I (its Sect. 3.4), there is scant evidence for significant variation in the overall luminosity of WR 140. Recently, Panov et al. (2000) monitored WR 140 from 1991 to 1998 in *UBV* photometry. In 1993 they observed a dip in the light curves of all three passbands around periastron passage, with a V-amplitude of 0.03 mag.

In the ultraviolet, Paper I sampled the flux level of the line-free UV continuum around 1800 Å from low resolution *IUE* spectra available at that time. Here we use the 35 absolute flux calibrated *IUE* spectra of WR 140 retrieved from the INES system (Cassatella 2000). From 34 spectra (excluding the overexposed SWP-9492), we measured a mean flux level of $7.8 \pm 0.2 \times 10^{-12}$ erg s^{-1} cm^{-2} Å^{-1}. The flux levels are plotted against

Table 2. Orbital parameters of WR 140 from this UV RV solution and from the optical RV solution of Paper I.

orbital parameters		Paper I (optical)	this study (UV)	weighted mean (optical+UV)
(1)		(2)	(3)	(4)
P	(d)	$2900^a \pm 10$		
$T_{\rm periastron}$	(JD 2 440 000+)	$9060^b \pm 29$	8956 ± 117	9054 ± 34
$T_{v_{\rm max}}$	(JD 2 440 000+)		8947 ± 117	
e		0.84 ± 0.04	0.87 ± 0.05	0.85 ± 0.04
ω	(°)	32 ± 8	31 ± 9	32 ± 8
γ	(km s^{-1})	-0.4	$23^c \pm 1$	
$K_{\rm O\,star}$	(km s^{-1})	28 ± 3	25 ± 15	28 ± 3
$a_{\rm O\,star} \sin i$	(AU)		3.29	
$f(M)$	($M_\odot$)		0.56	
reduced χ^2			2.37	
rms	(km s^{-1})		3.47	

Notes: *a*: IR photometric period. *b*: $6160 \pm 29 + 2900$ d. *c*: relative to HD 96715.

orbital phase in Fig. 3. The amplitude of the scatter is ∼8%, and, as in Paper I, we have to regard variation as unproven. However, the statistically insignificant UV flux dip of ∼6% at $\phi \simeq 0.95$, i.e., close to periastron, coincides partly with the much broader optical dip of $\Delta V = 0.03$ mag found by Panov et al. (2000). They interpreted that dip, which is too broad for a stellar eclipse, in terms of an "eclipse" by dust condensation in the WR-wind, of the type reported by Veen et al. (1998) for a number of late WC stars.

3.3. The luminosity of the O component

We compare the WR 140 WC7pd+O4-5 *IUE* spectrum with that of the single WC star WR 90 in Willis et al. (1986), and with those of single O4-5 stars presented in Walborn et al. (1985). We measured the equivalent widths of absorption and emission parts of the P-Cygni profiles at around 1400 Å (Si IV) and 1720 Å (N IV), and list them in Table 3.

WR 140 shows a strong Si IV λλ 1394,1403 Å P-Cygni resonance doublet and a weak N IV λ 1719 Å P-Cygni profile (see Fig. 5).

O-type stars show a P-Cygni feature at around 1720 Å due to N IV λ 1719 Å. This feature is strongest in O-type supergiants, moderate in O-type giants, and weakest in O-type main-sequence stars. The single O-type supergiants ζ Pup (O4I(n)f), HD 190429A (O4If$^+$) and HDE 269698 (O4If$^+$) show indeed strong N IV λ 1719 Å P-Cygni and strong Si IV P-Cygni resonance doublet components. The single O-type giants HD 15558 (O5III(f)) and HDE 269810 (O3III(f*)) have weak N IV and very weak SiIV P-Cygni resonance lines. The single O-type main-sequence stars 9 Sgr (O4V((f))), HD 46223 (O4V((f))) and HD 96715 (O4V((f))) show weak N IV absorption and no SiIV P-Cygni resonance lines.

We observe that the λ 1719 Å P-Cygni profile in the *IUE* spectra of WR 140 has an emission/absorption ratio of 20 and that of WR 90 has a ratio of 12. The O-type stars in Table 3 have ratios in the range ∼0.2–0.5. Therefore, we suggest that in the case of WR 140 the contribution of the O-companion to that line is only minor and thus more likely from an O-type main sequence star than a supergiant, where the latter have stronger 1719 Å lines than the former.

The Si IV P-Cygni profile of WR 140 almost exactly matches that of the single WC7 star WR 90 (see Willis et al. 1986) in its strong emission/absorption ratio of ∼1.3, while the O-type stars in Table 3 have ratios in the range ∼0.3–0.4. This indicates that in WR 140 the Si IV P-Cygni resonance-line originates mainly in the WC7 component.

From the comparisons made above, we conclude that the O-type component of WR 140 is more likely a main-sequence star.

An alternative way to determine the luminosity of the O component is provided by van der Hucht (2001). By comparing the equivalent widths of the C IV λ5808 Å, C III λ4650 Å, C III λ5696 Å and O III/IV λ5592 Å emission lines of WR 140 with those of the five apparently single WC7 stars WR 14, WR 50, WR 56, WR 68, and WR 90 (Conti & Massey 1989; Smith et al. 1990), he found for WR 140 that $\Delta M_v = M_v^{\rm comp} - M_v^{\rm WC7} = -0.6 \pm 0.3$. From a study of galactic WR stars in open clusters and OB associations, he derived that $M_v^{\rm WC7} = -4.5 \pm 0.7$ for single WC7 stars. Thus $M_v^{\rm comp} = -5.2 \pm 0.5$. This corresponds to the luminosity of a O3-8 V star or a O6.5-7 III star (Vacca et al. 1996), consistent with the result derived above.

3.4. Statistical significance of the observed variability

The UV spectra of WR 140 show variations with orbital phase, because the lines-of-sight towards the two binary

Table 3. Equivalent widths W_λ of the λ1400 Å and λ1720 Å P-Cygni emission and absorption features in WR 140, at $\phi = 0.5$ when wind-wind interaction is expected to be at a minimum, and in single WC7 and O3-5 stars.

star	spectral type	SWP no.	1400 Å abs. W_λ (Å)	1400 Å em. W_λ (Å)	1720 Å abs. W_λ (Å)	1720 Å em. W_λ (Å)
WR 140	WC7pd+O4-5	35886	9.6 ± 0.3	-12.5 ± 0.32	0.3 ± 0.1	-5.9 ± 0.3
WR 90	WC7	15130	11.0 ± 0.4	-14.5 ± 0.48	1.0 ± 0.2	-12.2 ± 0.7
ζ Pup	O4I(n)f	36143	6.0 ± 0.2	-2.0 ± 0.23	4.4 ± 0.2	-2.9 ± 0.2
HD 190429A	O4If$^+$	38994	6.5 ± 0.4	-2.0 ± 0.48	4.2 ± 0.5	-1.8 ± 0.3
		39006	6.8 ± 0.5	-2.1 ± 0.49	4.2 ± 0.5	-1.7 ± 0.3
HDE 269698	O4If$^+$	06967	5.1 ± 0.5	-1.3 ± 0.39	3.3 ± 0.4	-2.0 ± 0.4
		08011	4.8 ± 0.5	-1.1 ± 0.56	4.8 ± 0.5	-1.9 ± 0.3
HDE 269810	O3III(f*)	10755	0.8 ± 0.3	—	0.4 ± 0.2	-0.8 ± 0.3
HD 15558	O5III(f)	08322	3.7 ± 0.4	-1.0 ± 0.34	2.9 ± 0.4	-1.2 ± 0.3
9 Sgr	O4V((f))	15307	1.2 ± 0.2	-0.7 ± 0.23	2.3 ± 0.2	-0.5 ± 0.1
		38730	1.2 ± 0.2	-0.0 ± 0.27	2.0 ± 0.2	-0.5 ± 0.1
HD 46223	O4V((f))	10757	1.1 ± 0.6	-0.3 ± 0.74	2.4 ± 0.3	-0.7 ± 0.5
HD 96715	O4V((f))	22000	0.7 ± 0.3	-0.4 ± 0.30	2.9 ± 0.4	-0.5 ± 0.4

components probe at different times different regions of the O-star wind, the WR wind and the shock cone of the wind-wind collision region between the two stars.

The significance level of variability in our spectra is expressed in a Temporal Variance Spectrum (*TVS*), following Fullerton et al. (1996). In this method the observed variance in flux in each wavelength bin (0.1 Å) is compared to the variance due to instrumental and photon noise (at a corresponding flux level). The *TVS* can be approximated by:

$$(TVS)_\lambda \simeq \frac{1}{(N-1)} \sum_{i=1}^{N} \left[\frac{F_i(\lambda) - F_{\rm av}(\lambda)}{\sigma_i(\lambda)} \right]^2, \qquad (1)$$

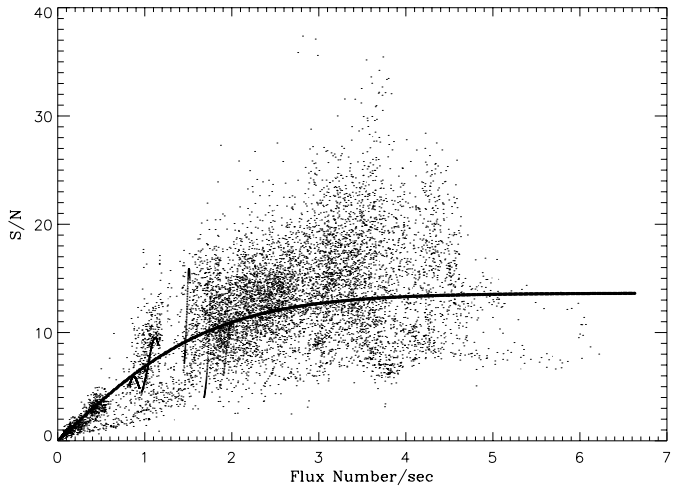

Fig. 4. *Dots:* S/N ratio as a function of $F(\lambda)$ determined from 35 *IUE*-SWP spectra of WR 140 at 4134 different wavelengths. *Curve:* best fit of a two-parameter function, see Eq. (2).

where N is the number of spectra, $\sigma_i(\lambda)$ is the standard deviation due to instrumental and photon noise, $F_i(\lambda)$ is the flux of the ith spectrum and $F_{\rm av}(\lambda)$ is the average spectrum.

The problem is to determine σ_i. Henrichs et al. (1994) found that for *IUE* spectra σ_i can be expressed as a function of flux only, by measuring the standard deviation of a set of spectra in each wavelength bin, excluding regions containing the variable spectral lines or where the echelle orders do not properly overlap. The ratio of $F_{\rm av}(\lambda)$ over $\sigma(\lambda)$, representing the S/N ratio, is fit with the function (see Fig. 4):

$$(S/N)_{\rm av} = (13.6 \pm 0.1) \quad \tanh\left(\frac{F}{1.8 \pm 0.05} \right). \qquad (2)$$

This function is used to specify σ_i for a given F_i in Eq. (1). To calculate the error in the S/N, we assumed a Poisson-distribution giving a reduced $\chi^2 = 1.0$. The asymptotic value of $S/N = 13.6$ fits our spectra best. We used the fit-function above to represent the S/N of all available WR 140 *IUE* spectra, and to calculate the $\sigma_i(\lambda)$. Next, we calculated the *TVS* value. Subsequently, we derived the Temporal Sigma Spectrum (TSS), which can be approximated by $\sqrt{TVS}$. This TSS can be considered as the ratio of the observed ($\sigma_{\rm obs}$) to the expected ($\sigma_{\rm exp}$) standard deviation and is a direct measure of the amplitude (and significance) of the variability.

The average spectrum and the corresponding σ-ratio of the *IUE*-SWP spectra of WR 140 are shown in Fig. 5. Only the strongest features are identified. More complete spectral line identifications of WC7 emission features are listed by Willis et al. (1986) for the single WC7 star WR 90 (HD 156385). In the available spectral regions,

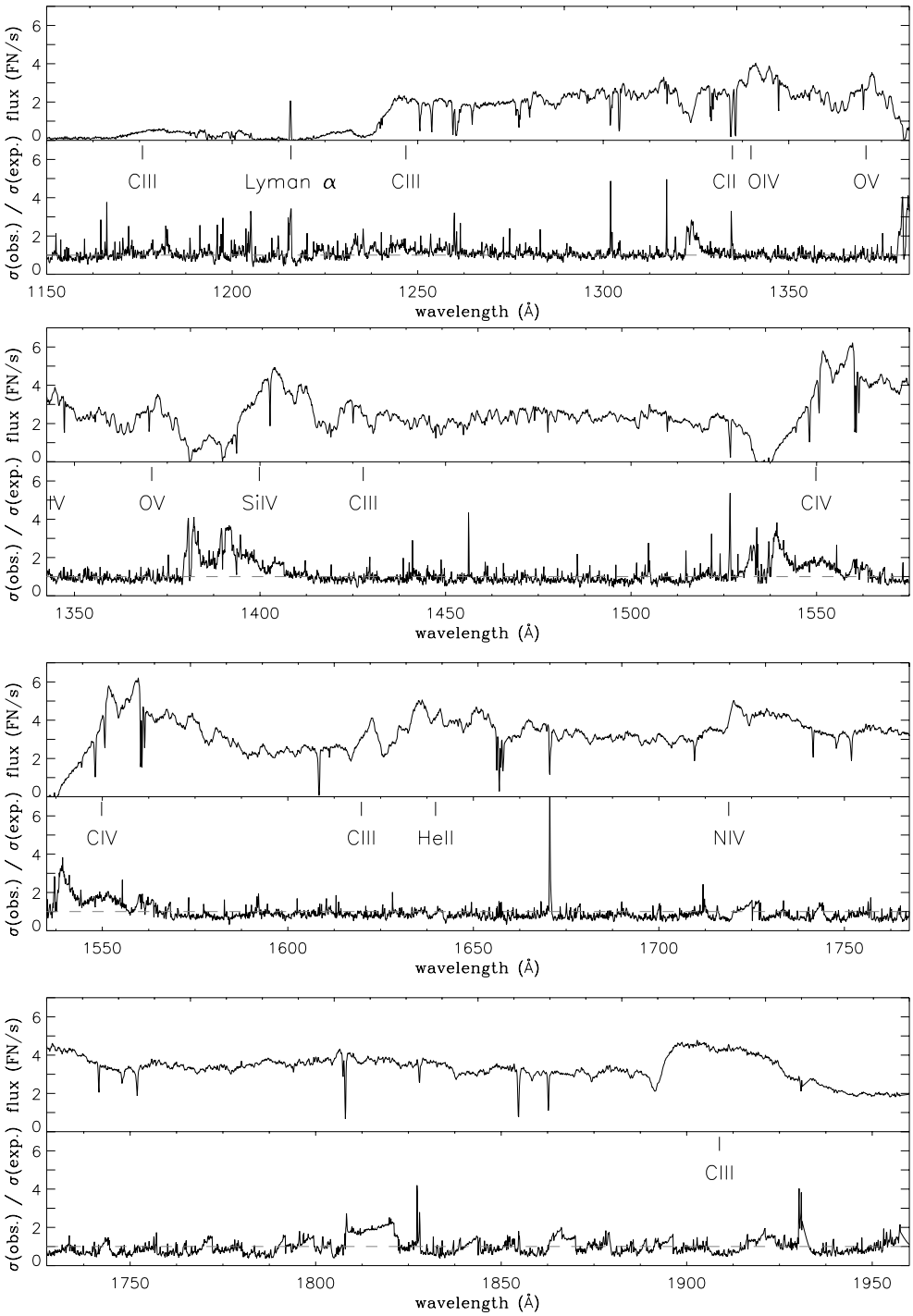

Fig. 5. *Upper panels*: average of 35 WR 140 *IUE*-SWP spectra sampled at 0.1 Å resolution in the 1150–1960 Å range. Relevant variable features are visible at $\lambda\lambda$ 1330 Å, 1400 Å and 1550 Å, corresponding to the resonance lines of C II, Si IV and C IV, respectively. Sharp absorption features are of interstellar origin. *Lower panels*: the Temporal Sigma Spectrum (TSS), i.e., the corresponding σ-ratio, with amplitude characterizing the variability (Sect. 3.4). Slight mismatches in wavelength calibration introduce peaks in the TSS, especially at the position of sharp lines.

$\sigma_{\rm obs}/\sigma_{\rm exp} > 1$ indicates variability. The larger the ratio, the stronger the degree of variability. We observe strong, broad variability around $\lambda\lambda$ 1330 Å, 1400 Å and 1550 Å. Those wavelength regions correspond to the resonance lines of C II, Si IV and C IV, respectively, and are discussed below.

3.5. Variable P-Cygni resonance line profiles

3.5.1. Lines present

All available spectra were scaled to the same flux level by conserving the total flux in the wavelength regions $\lambda\lambda$1435−1500 Å, 1565–1605 Å and 1740–1840 Å, where the

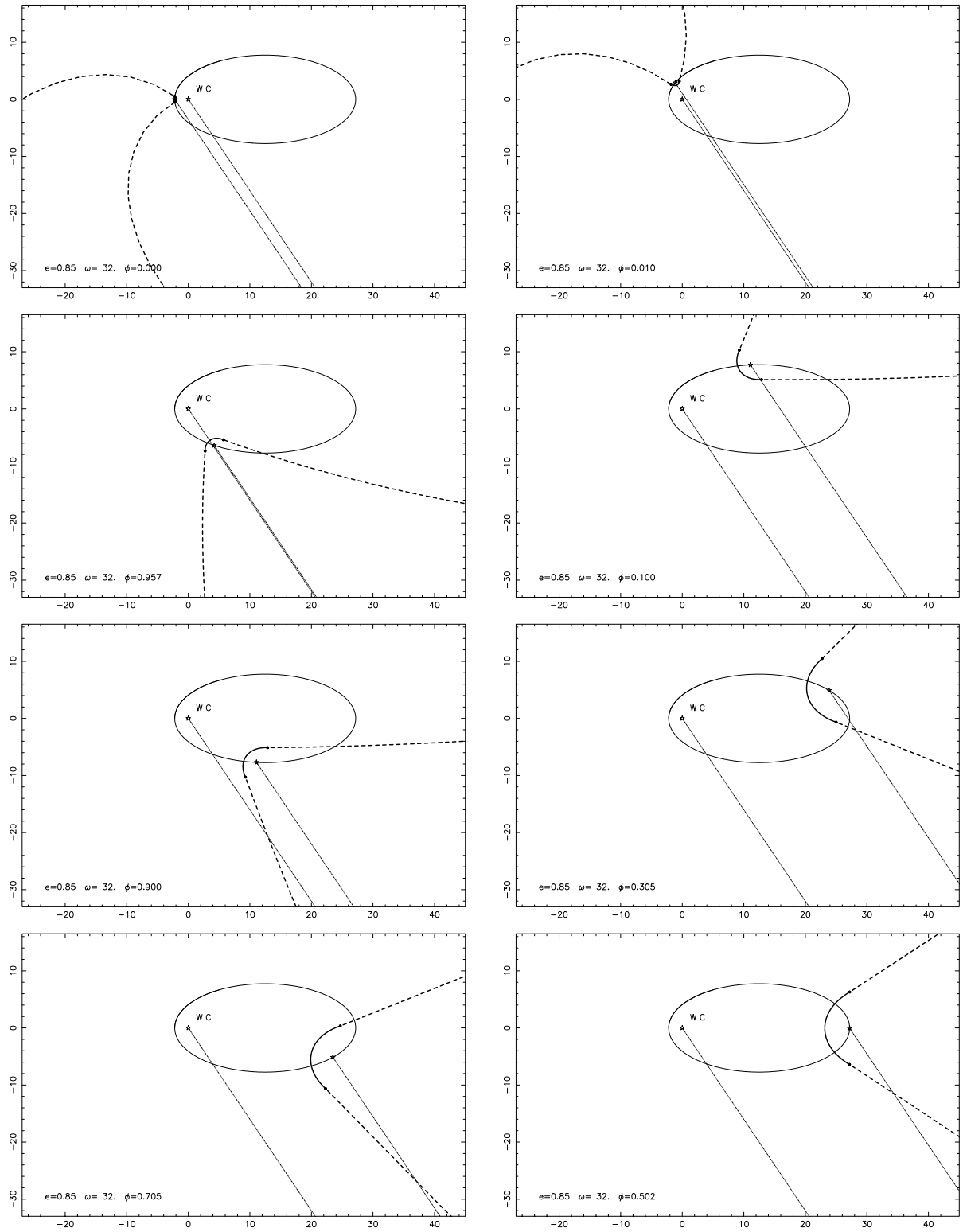

Fig. 6. Configurations of the WR 140 system as a function of phase shown in the plane of the orbit and reference frame of the WC component (marked). The O4-5 star orbits clockwise in this illustration, as does the wind-interaction region, marked by the contact discontinuity between the WC and O stellar winds. The form of the contact discontinuity is determined from the momenta of the two winds (Eichler & Usov 1993) and the relative velocities of the stellar winds and orbital motion. The changing sightlines to the two stars are shown.

spectra have relatively few features. In Fig. 8 we show a dynamic spectrum of the UV resonance doublet of C II $\lambda\lambda$1335,1336 Å, in Fig. 9 that of Si IV $\lambda\lambda$1394,1403 Å, and in Fig. 10 that of C IV $\lambda\lambda$ 1548,1551 Å, all in grey-scale representation. The orbital phase at the time of each observation is indicated by an arrow along the vertical scale.

The horizontal scale represents the velocity with respect to the rest wavelength of the principal doublet line. Strong variations occur in the absorption parts of the P-Cygni profiles around periastron passage ($\phi = 0$, see Fig. 2 for the geometry of the system).

3.5.2. Lines varying

In order to visualize the changing sightlines to the two binary components as a function of orbital phase, we plot in Fig. 6 eight different configurations, with increasing phase running clockwise. For most of the orbit, the WC star is observed through its own wind. Only around conjunction ($\phi = 0.957$), the phase interval depending on the orbital inclination and the opening angle of the wind-collision cone, can the sightline pass through the O star wind instead of the outer reaches of the WC wind. The O-type star, on the other hand, is observed through both part of the O stellar wind and, apart from a phase interval around conjunction, a varying sightline through the WC stellar wind whose optical depth and velocity range depend on phase. Because the O-type star is the brighter component and the WC wind has the greater optical depth, these variations have a significant influence on the observed spectrum. We note the following situations:

(1) Quadratures occur at $\phi = 0.996$ and 0.114. Between these phases, the O star is more distant than the WC star and is observed through both red-shifted and blue-shifted WC wind material. Both the velocity and the optical depth are at maximum at $\phi = 0.008$ and the effects of this are clearly seen in the Si IV and C IV observations (Figs. 7, 9, 10).

(2) From $\phi = 0.114$ to about $\phi = 0.5$, and depending on the inclination of the orbit, the sightline to the O-star passes through less of the WC stellar wind. At the same time, as the angle between the sightline and the wind falls, the velocity range covered by the P-Cygni absorption falls and approaches the terminal wind velocity. This is also seen in the evolution of the absorption features, particularly Si IV. This is consistent with the view (Sect. 3.3 and Table 3) that the Si IV is formed mainly in the WC7 star.

(3) As the orbit progresses, this evolution continues until $\phi \geq 0.85$ (depending on orbital inclination), our sightline to the WC7 star also passes through the O star wind until conjunction at $\phi = 0.957$. Our spectrum at this phase (SWP 46119) is not of the highest quality but the Si IV absorption does appear to be weakest at this phase.

3.5.2.1. Line-eclipse spectra

In order to visualize what happens around periastron, we took the ratio of the C II, Si IV and C IV profiles observed at $\phi = 0.010$ (O star *behind* the WR star in the line-of-sight, see Fig. 6) over the average of the 19 spectra observed at $0.5 < \phi < 1.0$ (O star *in front* of the WR star wind in the line-of-sight). We verified that all spectra between $\phi \simeq 0.5$ and $\phi = 0.957$ are almost similar. The result,

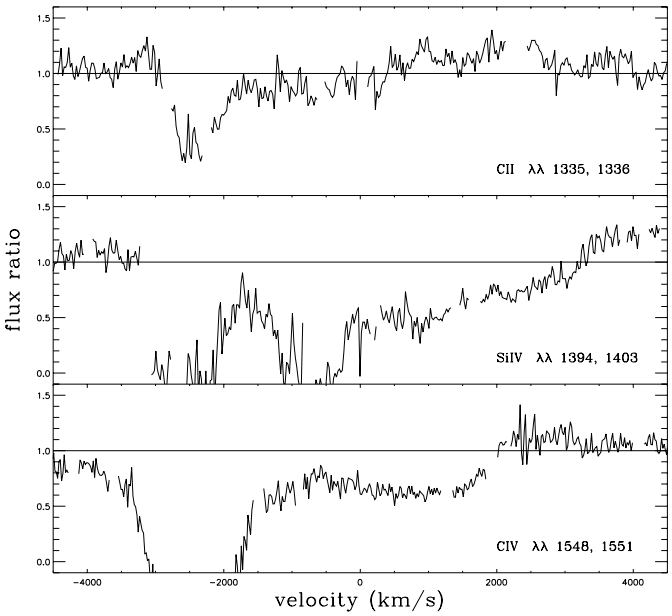

Fig. 7. Ratio of the *IUE* spectrum of WR 140 at $\phi = 0.010$ (O star *behind* the WR star in line-of-sight) and the average of 19 *IUE* spectra of WR 140 with $0.5 < \phi < 1$ (O star *in front* of the WR star wind in line-of-sight, see Fig. 2) for the C II, Si IV, and C IV resonance lines, giving "eclipse" spectra.

displayed in Fig. 7, shows "eclipse" spectra in those lines at phase $\phi = 0.010$, i.e., very close to periastron. We observe again that the C IV and Si IV resonance lines show at periastron excess absorption with $v_{\rm black} \simeq -3200$ km s^{-1}, i.e., $\sim$400 km s^{-1} faster than at quiescence.

The excess UV absorption occurs at the same phases as the excess X-ray absorption (Paper I).

The broad, shallow absorption features in the Si IV and C IV ratios are formed in the red-shifted WC wind material as noted above. The Si IV profile extends to about +3400 km s^{-1}, interpreted as a red shift of the λ 1403 Å component by +1250 km s^{-1}. The profile shows a discontinuity near this velocity which we attribute to the redshift of the stronger λ 1394 Å component. Similarly, we interpret the +2000 km s^{-1} redward extension of the C IV profile as a red shift of the λ 1551 Å component by +1500 km s^{-1}. These redshifts are interpreted as the maximum component of the WC stellar wind in our sightline to the O star and can be used to estimate the inclination of the orbit. Assuming no radiative braking, the maximum velocity is $v_\infty \sin(i - \theta_1)$, where i is the orbital inclination and θ_1 the angle above the orbital plane subtended at the WC star by the intersection of the sightline and the wind contact discontinuity. The value of θ_1 is found from i and the wind parameters using Eq. (24) of Cantó et al. (1996) to be $\theta_1 \simeq 10°$. A +1350 km s^{-1} maximum redshift then implies an orbital inclination $i = 38°$. Owing to the difficulty of fitting the absorption profiles, this may be a lower limit, but does suggest either that the orbit of WR 140 is not greatly inclined, or that radiative breaking of the WC stellar wind does occur at this phase.

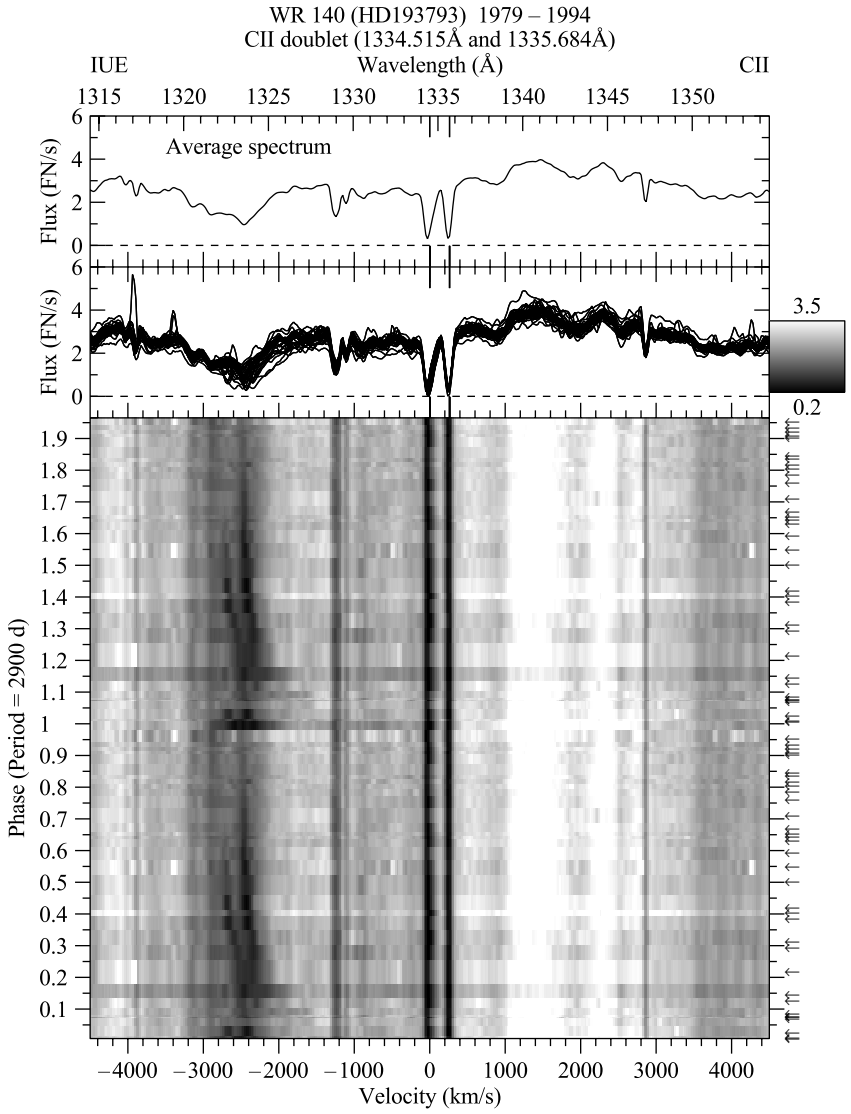

Fig. 8. The C II resonance doublet of WR 140 in grey-scale representation. Epochs of observation are indicated by arrows. The horizontal scale represents velocity with respect to the rest-wavelength of the principal doublet component. The interstellar doublet components of the C II resonance line mark the rest-wavelengths. At periastron ($\phi = 0$), the absorption troughs of the P-Cygni profiles become deeper and broader. The spectrum at $\phi = 0.406$ (SWS9492) is overexposed.

3.5.2.2. The C II $\lambda\lambda$1335,1336 Å resonance lines

The time-variable C II resonance P-Cygni line profiles (Fig. 8) show a significant non-variable narrow absorption dip in both doublet components at a constant velocity of about –3100 km s^{-1}, reminiscent of the narrow absorption components seen in O-type stars (Kaper et al. 1996). These represent very likely the signature of the terminal wind velocity of the O component.

Although the absorption part of the *red* doublet component is contaminated by the emission part of the *blue* doublet component, we observe for both doublet components a similar tendency of variability: the absorption features are broader and deeper right after periastron passage ($\phi = 0$).

At the *blue* end of these absorption features we measure $v_{\rm black} \simeq -2800$ km s^{-1} at all phases. At periastron passage no change in $v_{\rm black}$ is observed, contrary to what happens in the C IV and Si IV resonance line profiles (see below). However, at periastron the *red* black-edge of the C II P-Cygni absorption trough abruptly expands from about –2800 km s^{-1} to –1800 km s^{-1}. The *red* black-edge of the C II absorption trough is back to quiescence at $\phi \simeq 0.6$, when the the line-of-sight passes through rather more of the O star wind and less of the WC stellar wind (see Fig. 6).

3.5.2.3. The Si IV $\lambda\lambda$1394,1403 Å resonance lines

Although the absorption part of the *red* doublet component is contaminated by the emission part of the *blue* doublet component, we observe for both Si IV doublet components a similar tendency of variability: the absorption

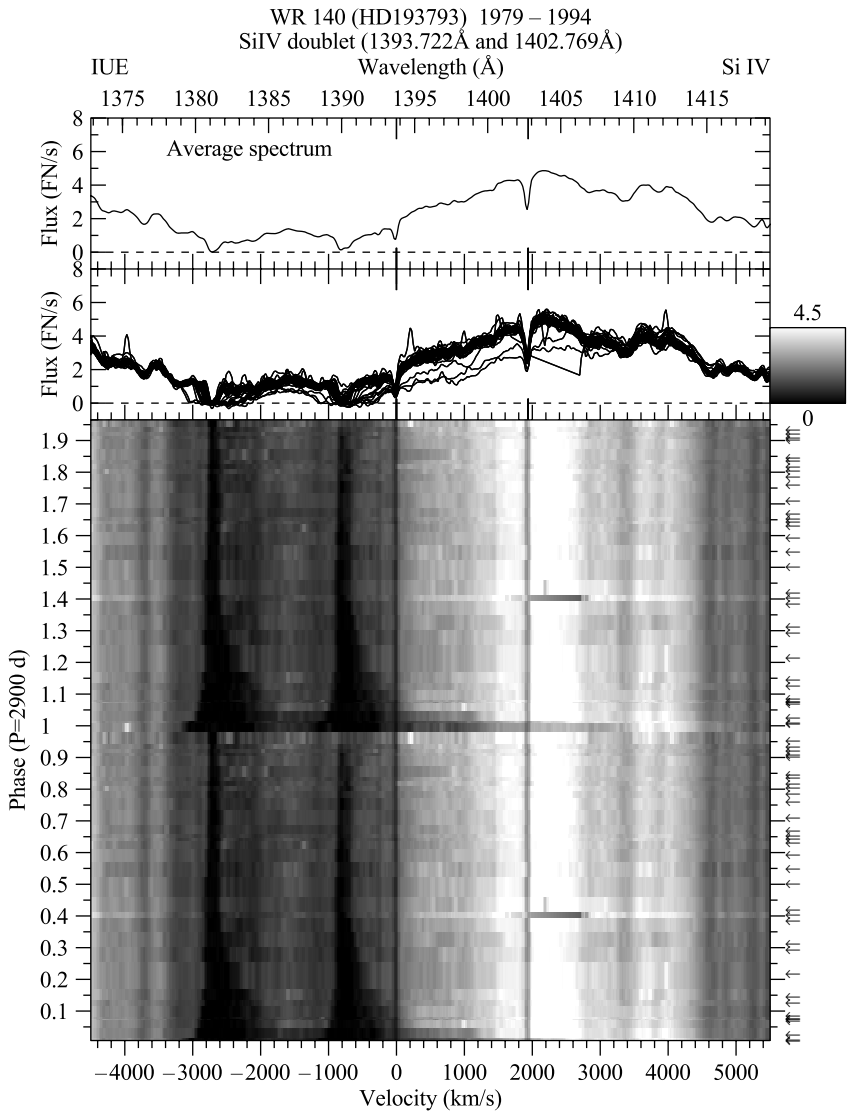

Fig. 9. The same as Fig. 8, here for Si IV.

features are broader and deeper right after periastron passage ($\phi = 0$), and even become saturated.

At the *blue* end of these absorption features we measure $v_{\rm black} \simeq -2800$ km s^{-1} for $0.3 < \phi < 0.96$, i.e., during quiescence. Just after periastron passage ($\phi = 0$), $v_{\rm black}$ increases abruptly to about –3200 km s^{-1}. At phase $\phi \simeq 0.3$, $v_{\rm black}$ has gradually returned back to about –2800 km s^{-1}.

Also just after periastron passage, the *red* black-edge of the Si IV P-Cygni absorption trough abruptly expands from about –2600 km s^{-1} to about –2000 km s^{-1}. Thus, at $\phi \simeq 0$ the Si IV black absorption trough has a total extent from about –3200 to –2000 km s^{-1}. In addition, as can be seen clearly in Fig. 9, overall excess *red* absorption extends to +3400 km s^{-1}.

The *blue* black-edge of the Si IV absorption trough is back to quiescence at $\phi \simeq 0.2$; the *red* black-edge of the Si IV absorption trough is back to quiescence at $\phi \simeq 0.4$.

The time-variable Si IV resonance P-Cygni line profiles (Fig. 9) show a significant non-variable narrow absorption feature with approximately the same wavelength separation as the Si IV doublet components at a constant wavelength, corresponding to a Si IV velocity of about −3700 km s^{-1}. However, since at that velocity no absorption features are seen in other P-Cygni profiles of WR 140, these absorption features must be of O star photospheric origin.

3.5.2.4. The C IV λλ 1548,1551 Å resonance lines

Although the absorption troughs of both C IV doublet components largely overlap, we observe for both a similar tendency of variability: the saturated absorption features are broader right after periastron passage ($\phi = 0$).

At the *blue* end of these absorption features we measure $v_{\rm black} \simeq -2800$ km s^{-1} for $0.6 < \phi < 0.96$, i.e., during quiescence. Just after periastron passage, $v_{\rm black}$ increases abruptly to about –3200 km s^{-1}. At phase $\phi \simeq 0.6$, $v_{\rm black}$ has gradually returned back to about –2800 km s^{-1}.

Also at periastron the *red* black-edge of the C IV P-Cygni absorption trough abruptly expands from about

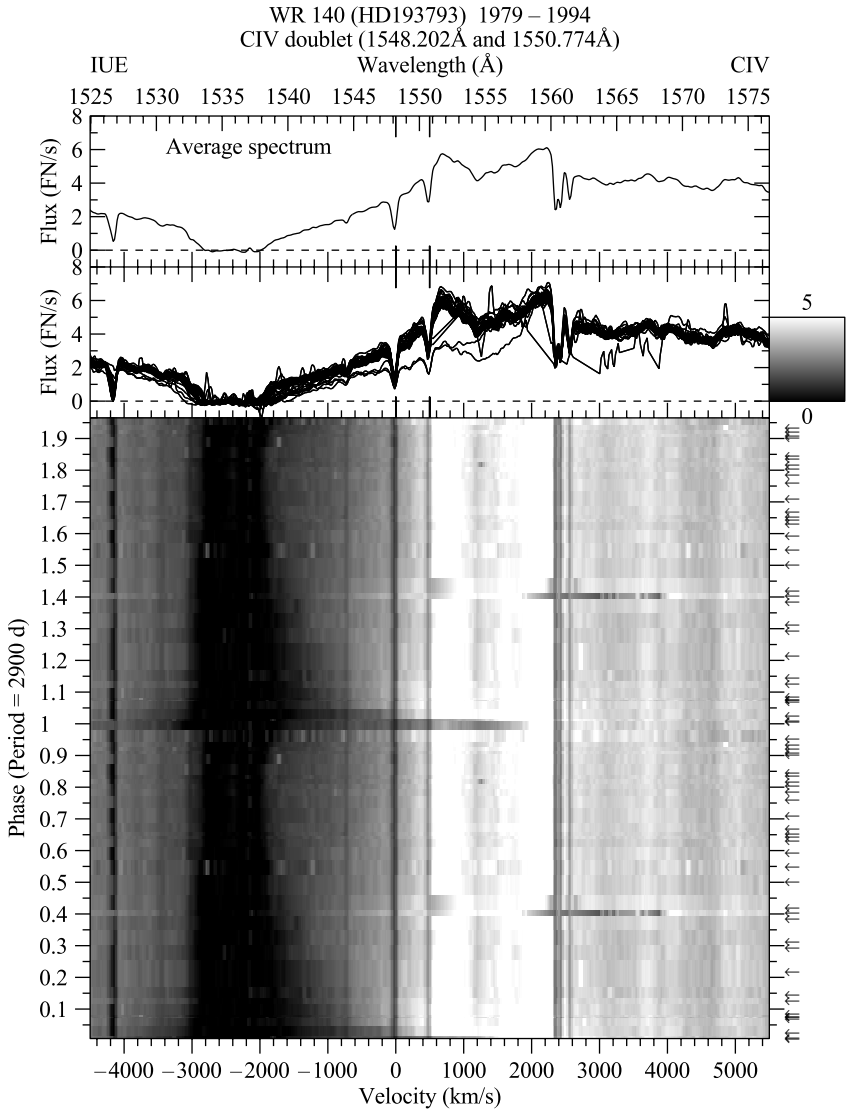

Fig. 10. The same as Fig. 8, here for C IV. The strong narrow absorption feature at 1527 Å is Si II λ1526.71 Å.

–2600 km s^{-1} to about –1700 km s^{-1}. Thus, at $\phi \simeq 0$ the C IV black absorption width has a total extent from about –3200 to –1700 km s^{-1}. In addition, as can be seen clearly in Fig. 10, overall excess *red* absorption extends to +2000 km s^{-1}.

The *blue* and *red* black-edges of the C IV absorption trough are back to quiescence at $\phi \simeq 0.6$. when the line-of-sight passes through rather more of the O star wind and less of the WC stellar wind (see Fig. 6).

The time-variable C IV resonance P-Cygni line profiles (Fig. 10) show a faint non-variable narrow absorption feature in both doublet components with approximately the same wavelength separation as the C IV doublet components at a constant wavelength difference, corresponding to a C IV velocity of about –3400 km s^{-1}. However, since at that velocity no absorption features are seen in other P-Cygni profiles of WR 140, these absorption features must be of O star photospheric origin. *IUE* spectra of single OV-type stars show absorption features at the same wavelengths (Walborn 1985).

It appears that the C II, C IV and Si IV resonance lines behave identically, the difference being the optical depth.

3.5.2.5. Other spectral lines

At 1640 Å, the wavelength of the strongest He II emission line, we find no significant variability. In contrast, *IUE* spectra of the WN binaries HD 90657 (WR 21, WN5+O4-6), V444 Cyg (WR 139, WN5+O6III-V), and GP Cep (WR 153, WN6/WCE+O6I) show variable He II λ1640 Å emission-line strength when the O star is *in front* of the WR star in the line-of-sight (Koenigsberger & Auer 1985).

We also looked for variability in the N V λλ 1239,1243 Å resonance doublet, which we expect to be observable from the O-star wind only. Unfortunately, this line is blended

by the absorption part of the WC C III λ 1247 Å P-Cygni profile (not a resonance line, not variable) and the S/N ratio is rather low in this part of our *IUE* spectra.

4. Discussion

4.1. WR 140

In general, when the inclination of a WR+O colliding wind binary causes wind occultation effects, we can expect the observed wind velocities reflected in the blue black-edges of the P-Cygni absorption troughs to vary between the wind terminal velocities of the individual WR star and O star.

In the absorption part of the Si IV P-Cygni profile (Fig. 9), the *blue* black-edge of the absorption trough, i.e., the apparent terminal wind velocity, increases by $\Delta v_\infty \simeq 400$ km s^{-1} to $v_\infty \simeq 3200$ km s^{-1}, when the O star in its orbit passes the WC star at periastron ($\phi \simeq 0$) and moves behind it in the line-of-sight (see Fig. 6). In Sect. 3.3 we concluded that the Si IV $\lambda\lambda$ 1394,1403 Å resonance-line doublet originates only in the WC7 star. Even if the O component contributed to that line, the increase to maximum *blue*-shifted velocity of –3200 km s^{-1} at $\phi = 0$ cannot have been caused in the O star wind alone, because the O star *wind* provides less absorption than the much denser WC star wind. The O star *light* in the line-of-sight at $\phi = 0$ is being absorbed by both the O-star wind and the WC-star wind matter. Thus the apparent Δv_∞ occurs when the line-of-sight to the O star passes very close to the WC star through the WC wind.

Contrary to this, the C II $\lambda\lambda$ 1335,1336 Å and C IV $\lambda\lambda$ 1548,1551 Å resonance lines originate in both binary components. This can be seen clearly in the C II profile (Fig. 8), where two sets of shifted doublet components are present. One set is blue-shifted by about –2800 km s^{-1}, and the other set, slightly fainter, is blue-shifted by about –3100 km s^{-1}. The set with higher velocity shows a consistent brightness throughout the orbit while the set with lower velocity shows variability. The absorption profile is very broad just after periastron and gradually becomes narrower until around phase $\phi \simeq 0.4-0.6$, whereafter the absorption trough becomes relatively weak. The larger velocity is reminiscent of the terminal wind velocities $v_\infty \simeq 3200$ km s^{-1} for O4-5 stars (Conti 1988). The smaller velocity is consistent with the observations of WR 140 by Eenens & Williams (1994), who measured v_∞(He I 1.083 μm) = 2900 km s^{-1} and v_∞(He I 2.058 μm) = 2845 km s^{-1}, respectively.

Again, we emphasize that the variability is observed as excess absorption, i.e., in the absorption troughs of the P-Cygni line profiles of C II, Si IV and C IV during and just after $\phi \simeq 0$, and over the whole P-Cygni profiles of Si IV and C IV. Thus the variations are related to changes in the lines-of-sight towards both stars. When the O star is *in front* of the WC wind ($0.6 \lesssim \phi \leq 0.957$, see Fig. 6), we observe in the line-of-sight towards the O star through material of the O-star wind *and*, superimposed, in the line-of-sight towards the WC star through much denser WC wind material (recall that the O-star wind is confined to a cone in the WC-star wind, see Fig. 6). For about half of the orbit after periastron ($0 < \phi \lesssim 0.6$), the dense WC wind is *in front* of the O star, dominating the absorption in the line-of-sight towards the O star. Thus, only when the O star is in *front* of the WC star in the line-of-sight ($\phi \simeq 0.8-0.9$), does one observe uncontaminated O-star material in the line-of-sight towards that component. Right after periastron passage ($0 < \phi \lesssim 0.1$), the bulk of the dense WC wind is in front of the O star in the line-of-sight, dominating the circumstellar absorption.

The observed asymmetric velocity increase/decrease is clearly caused by the large eccentricity of the orbit (as concluded in Sect. 3.1), both conjunctions are very close to periastron passage, occurring at $\phi = 0.957$ (O star in front) and $\phi = 0.010$ (O star behind), and the aspect angle, affecting the sightlines towards both binary components as a function of orbital phase.

The increase at periastron in maximum *blue* velocity (to about –3100 km s^{-1}) cannot be solely due to absorption in the O star wind (which has the larger wind velocity), because most of the absorption at these orbital phases occurs through the much denser (but slower) WC wind.

We offer the following explanations:

(*i*) At the stronger-absorption/larger velocity phases ($0 < \phi \lesssim 0.3$), the sightline to the (brighter) O star passes close to the WC star and through the densest part of its wind, where anomalously broad emission lines are formed (corresponding to ~4200 km s^{-1}, Torres et al. 1986). The manifestations of broadening may be caused by turbulence in the wind, probably arising from the wind-wind collision region.

(*ii*) If the WR wind is not spherically symmetric but faster at latitudes around the WR star's equator (likely to be aligned with the orbital plane), then faster sightline absorption due to wind occultation, as observed at $\phi = 0$, would be a logical consequence.

(*iii*) As a hypothesis, because the luminosity of the O star is about twice that of the WC star, the majority of the UV photons are emitted by the O star. Both stellar winds are driven by radiation pressure; when the separation between the two stars is smallest (the minimum separation is ~2.35 AU $\simeq 500\,R_\odot$, see Paper I) one could expect that common-envelope acceleration by the combined WC and O stellar radiation fields, which is always dominated by that of the O star, is most effective, since this effect scales with the squared separation of the binary components in their eccentric orbit. This, however, would have to be proven through atmospheric modelling, which is beyond the scope of this paper.

(*iv*) As a further hypothesis, recent investigations of Gayley (2001) indicate that in massive close binaries enhanced radiatively driven mass loss due to tidal stresses will be focused along the orbiting line of centers. Koenigsberger et al. (2001) explain the variability observed in HD 5980 by this effect.

Table 4. Observed terminal wind velocities and excess terminal wind velocities observed in the *IUE* spectra of WR 11, WR 137, WR 139, and WR 140.

star	WR 11		WR 137		WR 139		WR 140	
type	WC8+O7.5III-V		WC7pd+O9		WN5+O6III-V		WC7pd+O4-5	
e	0.33 ± 0.01		> 0.12		0.04 ± 0.01		0.85 ± 0.04	
i (°)	63 ± 8				78.7±0.5		> 38	
ω (°)	68						31 ± 9	
	$v_\infty^{\rm WR}$	Δv_∞	$v_\infty^{\rm WR}$	Δv_∞	$v_\infty^{\rm WR}$	Δv_∞	$v_\infty^{\rm WR}$	Δv_∞
	($\rm km\,s^{-1}$)		($\rm km\,s^{-1}$)		($\rm km\,s^{-1}$)		($\rm km\,s^{-1}$)	
resonance lines	1450	500	1900	300	1700	1200	2800	400

Note: Stellar parameters are from the compilation of van der Hucht (2001), except for WR 140 and WR 137, which are from this study.

4.2. Other Wolf-Rayet colliding wind binaries

The literature provides data on some other WR colliding wind binaries that show excess wind velocities as a function of orbital phase:

(*a*) The long-period WC7pd+O9 binary WR 137, with a period of $P = 13.1$ yr (Williams et al. 2001), shows in its *IUE*-SW spectra a behaviour similar to that of WR 140, with an excess $\Delta v_\infty \simeq 300$ $\rm km\,s^{-1}$ at periastron.

(*b*) The apparent wind variability phenomena in the *IUE* spectra of WR 140 (and WR 137) discussed above are reminiscent of those found by St-Louis et al. (1993) in *Copernicus* and *IUE* UV spectra of the WC8+O7.5III-V binary γ^2 Velorum (WR 11, $P = 0.22$ yr, $i \simeq 65°$). They argued that the pattern of variability in the UV spectra of γ^2 Vel can be understood in terms of selected eclipses of the O star light when passing through the WC8 stellar wind, as proposed by Willis & Wilson (1976), combined with an asymmetric wind density due to colliding wind effects. The same *IUE* data of WR 11 had been interpreted earlier by Brandi et al. (1989), who suggested that the variable v_∞ components observed in the Si IV, C IV and N V resonance line profiles of WR 11 are caused by a jet-stream of gas moving away from the system with a velocity of ~ -700 $\rm km\,s^{-1}$. Applying the correction factor of 0.76 of Prinja et al. (1990), this scales down to a jet outstream velocity of about –500 $\rm km\,s^{-1}$. A similar apparent outstream velocity variability in WR 11 has been observed in monitoring observations of the optical C III λ 4650 (non-resonance) *emission* line by Schweickhardt et al. (1999), who found that the variable component shows a maximum outstream velocity of about –700 $\rm km\,s^{-1}$.

(*c*) Variable excess *emission* components have also been observed in the C III λ 5696 *emission* lines of the short-period WC7+O binaries WR 42 ($P = 7.9$ d) and WR 79 ($P = 8.9$ d) by Hill et al. (2000), as a function of orbital phase. They assume, following Lührs' (1997) earlier study of that emission line in WR 79, that the excess emission arises in the colliding wind regions of the respective WC7+O binaries. In the analytical Lührs model it is assumed that the O star and its wind are embedded in the wind of the WR star, and that the boundary surface is cone-like and rotationally symmetric with respect to the line connecting the two stars. Model fitting of the observed excess emission profiles as a function of phase, allows one to obtain the streaming velocity $v_{\rm str}$ of material in the cone, among other cone parameters. For WR 42 Hill et al. (2000) find that $v_{\rm str} \simeq 1740\,\rm km\,s^{-1}$, while its $v_\infty = 1500$ $\rm km\,s^{-1}$ (Eenens & Williams 1994); for WR 79 they find that $v_{\rm str} \simeq 2000$ $\rm km\,s^{-1}$, while its $v_\infty = 2270$ $\rm km\,s^{-1}$ (Prinja et al. 1990). Apparently their streaming velocities are of the order of magnitude of the terminal wind velocities.

(*d*) *IUE* spectra of the short-period ($P = 4.2$ d) WN5+O6III-V close and eclipsing binary V444 Cyg show an excess terminal velocity of $\Delta v_\infty \simeq 1200$ $\rm km\,s^{-1}$ (from about –1700 to –2900 $\rm km\,s^{-1}$, but contrary to the three WC cases, only when the O-type star is *in front* of the WN star (Shore & Brown 1988, their wind velocities scaled down by a factor of 0.76 following Prinja et al. 1990).

(*e*) The extremely variable medium-period ($P = 19.3$ d, $e = 0.31$, $i = 88°$) LBV/WR eclipsing binary HD 5980 in the SMC shows only when star B (the WN4 star) is *in front* of star A (the LBV-type eruptor in the system), i.e., at the time of eclipse of star A, a sudden increase of the C IV P-Cygni absorption edge velocity from –2500 $\rm km\,s^{-1}$ to –3300 $\rm km\,s^{-1}$ (Koenigsberger et al. 2000).

Indications of enhanced, focused winds at periastron have also been found in OB binaries, e.g. in the medium-period ($P = 29.1$ d, $e = 0.764$) O9III+B1III binary ι Ori (Gies et al. 1996).

The case of WR 140 has also corresponding aspects with the massive binary η Car ($P = 5.52$ yr, $e = 0.90$) according to Corcoran et al. (2001), who argue for a phase-dependent mass loss from η Car near periastron, on the basis of its X-ray light curve.

In Table 4 we summarize the observed velocities from *IUE* studies of WR 11, WR 137, WR 139 and WR 140. We conclude for all cases, that the observed excess velocities in the spectra of these WR+O binaries are caused by variable absorption in the sightlines to the O stars when passing through their respective turbulent wind-wind collision regions. For the binaries with very eccentric orbits the

excess velocities could be enhanced by variable common envelope radiative acceleration.

5. Conclusions

From a study of a 35 high-resolution *IUE*-SW spectra of WR 140 (WC7pd+O4-5), we have derived a radial velocity solution, and we have shown the occurrence of substantial resonance line variations in this system. We draw the following conclusions:

1. The large eccentricity of the 7.94 yr orbit is confirmed at $e = 0.87$.

2. The O4-5 component is a main sequence star.

3. Significant changes in the shape of the UV line profiles and strengths are confined to resonance lines of ions expected to be chemically abundant in the WC7 and O4-5 stellar winds.

4. The detailed phase-dependent nature of the line profile changes is found to be consistent with the concept of selective line eclipses of the O4-5 star light by the WC7 stellar wind, affected strongly by the orbital geometry which determines the lines-of-sight to the individual binary components as a function of orbital phase.

5. While it appears clear that line-eclipsing effects are the main cause of the observed UV spectral variability, the detailed line profile changes show that at least some of the eclipsing material is not distributed in a spherically symmetric way around the WC7 star. This is considered to be due to a combination of: (*i*) interaction effects involving the collision of the two stellar winds, i.e., turbulence with a large velocity dispersion in the wind-wind collision zone; (*ii*) the possibility of an orbital-plane enhanced WC7 stellar wind velocity; (*iii*) possible common-envelope acceleration by the combined WC and O stellar radiation fields; and/or (*iv*) possible enhanced radiatively driven mass loss due to tidal stresses, focused along the orbiting line of centers.

Acknowledgements. Our thanks go to Wilhelm Seggewiss for his constructive and helpful referee report. We thank Michael Corcoran, Marten van Kerkwijk, Bob Koch, Gloria Koenigsberger, Andy Pollock and Ian Stevens for valuable critical comments on an earlier version of the manuscript. DYASG gratefully acknowledges financial support from The Rotary Foundation, the University of Utrecht, and the Leids Kerkhoven-Bosscha Fonds. LK is supported by a fellowship of the Royal Academy of Sciences of the Netherlands.

References

Annuk, K. 1995, in Wolf-Rayet Stars: Binaries, Colliding Winds, Evolution, ed. K. A. van der Hucht, & P. M. Williams (Dordrecht: Kluwer), Proc. IAU Symp., 163, 231
Arnal, E. M. 2001, AJ, 121, 413
Auer, L. H., & Koenigsberger, G. 1994, ApJ, 436, 859
Barker, P. K. 1984, AJ, 89, 899
Bianchi, L., & Bohlin, R. C. 1984, A&A, 134, 31
Brandi, E., Ferrer, O. E., & Sahade, J. 1989, ApJ, 340, 1091; Erratum: ApJ, 347, 561
Cantó, J., Raga, A. C., & Wilkin, F. P. 1996, ApJ, 469, 729
Cassatella, A., Altamore, A., González-Riestra, R., et al. 2000, A&AS, 141, 331
Cherepashchuk, A. M. 1976, Pis'ma Astron. Zh. 2, 356 (= Sov. Astron. Lett. 2, 138)
Conti, P. S. 1971, in Wolf-Rayet and High-Temperature Stars, ed. M. K. V. Bappu, & J. Sahade (Dordrecht: Reidel), Proc. IAU Symp., 49, 225
Conti, P. S., Roussel-Dupré, D., Massey, P., & Rensing, M. 1984, ApJ, 282, 693
Conti, P. S., & Massey, P. 1989, ApJ, 337, 251
Corcoran, M. F., Ishibashi, K., Swank, J. H., & Petre, R. 2001, ApJ, 547, 1034
Eenens, P. R. J., & Williams, P. M. 1994, MNRAS, 269, 1082
Eichler, D., & Usov, V. 1993, ApJ, 402, 271
Fitzpatrick, E. L., Savage, B. D., & Sitko, M. L. 1982, ApJ, 256, 578
Fleming, W. P. 1889, Astron. Nachr., 122, 159
Florkowski, D. R., & Gottesman, S. T. 1977, MNRAS, 179, 105
Fullerton, A. W., Gies, D. R., & Bolton, C. T. 1996, ApJS, 103, 475
Gayley, K. G. 2001, in Interacting Winds from Massive Stars, ed. A. F. J. Moffat, & N. St-Louis, Proc. Int. Workshop, Les Îles-de-la-Madeleine (Québec, Canada), 10–14 July 2000, ASP-CS, in press
Gies, D. R., Barry, D. J., Bagnuolo, W. G., Sowers, J., & Thaller, M. L. 1996, ApJ, 469, 884
Hackwell, J. A., Gehrz, R. D., Smith, J. R., & Strecker, D. W. 1976, ApJ, 210, 137
Henrichs, H. F., Kaper, L., & Nichols, J. S. 1994, A&A, 285, 565
Hill, G. M., Moffat, A. F. J., St. Louis, N., & Bartzakos, P. 2000, MNRAS, 318, 402
Howarth, I. D., Murray, J., Mills, D., & Berry, D. S. 1996, Starlink User Note 50.21
van der Hucht, K. A., Conti, P. S., Lundström, I., & Stenholm, B. 1981, SSR, 28, 227
van der Hucht, K. A. 1992, A&A, 4, 123
van der Hucht, K. A. 2001, New Astron. Rev., 45, 135
Kaper, L., Henrichs, H. F., Nichols, J. S., et al. 1996, A&AS, 116, 257
Koenigsberger, G., & Auer, L. H. 1985, ApJ, 297, 255
Koenigsberger, G., Georgiev, L., Barbá, R., et al. 2000, ApJ, 542, 428
Koenigsberger, G., Moreno, E., & Cervantes, F. 2001, in Interacting Winds from Massive Stars, ed. A. F. J. Moffat, & N. St-Louis, Proc. Int. Workshop, Les Îles-de-la-Madeleine (Québec, Canada) 10–14 July 2000, ASP-CS, in press
Lamontagne, R., Moffat, A. F. J., & Seggewiss, W. 1984, ApJ, 277, 258
Lührs, S. 1997, PASP, 109, 504
McDonald, J. K. 1947, Pub. Dom. Ap. Obs. Victoria, 7, 311
Moffat, A. F. J., & Shara, M. M. 1986, AJ, 92, 952
Panov, K. P., Altmann, M., & Seggewiss, W. 2000, A&A, 355, 607
Pollock, A. M. T. 1987, A&A, 171, 135
Prinja, R. K., Barlow, M. J., & Howarth, I. D. 1990, ApJ, 361, 607; Erratum: 1991, ApJ, 383, 466
Prinja, R. K. 1994, A&A, 289, 221
Rees, P., Giddings, J. R., & Clayton, M. 1996a, STARLINK Miscellaneous User Document 45.1
Rees, P., Giddings, J. R., Mills, D., & Clayton, M. 1996b, STARLINK Guide 3.5

Schumann, J. D., & Seggewiss, W. 1975, in Variable Stars and Stellar Evolution, ed. V. E. Sherwood, & L. Plaut (Dordrecht: Reidel), Proc. IAU Symp., 67, 299
Schweickhardt, J., Schmutz, W., Kaufer, A., Stahl, O., & Wolf, B. 1999, in Wolf-Rayet Phenomena in Massive Stars and Starburst Galaxies, ed. K.A. van der Hucht, G. Koenigsberger, & P. R. J. Eenens (San Francisco: ASP), Proc. IAU Symp., 193, 98
Setia Gunawan, D. Y. A., van der Hucht, K. A., Williams, P. M., et al. 1995a, in Wolf-Rayet Stars: Binaries, Colliding Winds, Evolution, ed. K. A. van der Hucht, & P. M. Williams (Dordrecht: Kluwer), Proc. IAU Symp., 163, 466
Setia Gunawan, D. Y. A., van der Hucht, K. A., Stickland, D. J., et al. 1995b, in Wolf-Rayet Stars: Binaries, Colliding Winds, Evolution, ed. K. A. van der Hucht, & P. M. Williams (Dordrecht: Kluwer), Proc. IAU Symp., 163, 508
Shore, S. N., & Brown, D. N. 1988, ApJ, 334, 1021
Smith, L. F., Shara, M. M., & Moffat, A. F. J. 1990, ApJ, 358, 229
Stickland, D. J., & Lloyd, C. 1990, Observatory, 110, 1
St-Louis, N., Willis, A. J., & Stevens, I. R. 1993, ApJ, 415, 298
Torres, A. V., Conti, P. S., & Massey, P. 1986, ApJ, 300, 379
Vacca, W. D., Garmany, C. D., & Shull, M. J. 1996, ApJ, 460, 914
Veen, P. M., van Genderen, A. M., van der Hucht, K. A., et al. 1998, A&A, 329, 199
Walborn, N. R., Nichols-Bohlin, J., & Panek, R. J. 1985, NASA RP-1155
White, R. L., & Becker, R. H. 1995, ApJ, 451, 352
Williams, P. M., van der Hucht, K. A., van der Woerd, H., et al. 1987, in Instabilities in Luminous Early Type Stars, ed. H. Lamers, & C. W. H. de Loore, Proc. Symp. in honour of C. de Jager (Dordrecht: Reidel), 221
Williams, P. M., van der Hucht, K. A., Pollock, A. M. T., et al. 1990, MNRAS, 243, 662 (Paper I)
Williams, P. M., van der Hucht, K. A., & Spoelstra, T. A. Th. 1994, A&A, 291, 805 (Paper II)
Williams, P. M. 1995, in Wolf-Rayet Stars: Binaries, Colliding Winds, Evolution, ed. K. A. van der Hucht, & P. M. Williams (Dordrecht: Kluwer), Proc. IAU Symp., 163, 335
Williams, P. M. 2001, in Interacting Winds from Massive Stars, ed. A. F. J. Moffat, & N. St-Louis, Proc. Int. Workshop, Les Îles-de-la-Madeleine (Québec, Canada) 10–14 July 2000, ASP-CS, in press
Williams, P. M., Kidger, M. R., van der Hucht, K. A., et al. 2001, MNRAS, 324, 156
Willis, A. J., & Wilson, R. 1976, A&A, 47, 429
Willis, A. J., van der Hucht, K. A., Conti, P. S., & Garmany, C. D. 1986, A&AS, 63, 417
Zhekov, S. A., & Skinner, S. L. 2000, ApJ, 538, 808